1-1-2017

Longitudinal assessment of metal concentrations and copper isotope ratios in the G93A SOD1 mouse model of amyotrophic lateral sclerosis

T. Gabriel Enge
University of Wollongong, tge571@uowmail.edu.au

Heath Ecroyd
University of Wollongong, heathe@uow.edu.au

Dianne F. Jolley
University of Wollongong, djolley@uow.edu.au

Justin J. Yerbury
University of Wollongong, jyerbury@uow.edu.au

Anthony Dosseto
University of Wollongong, tonyd@uow.edu.au

Longitudinal assessment of metal concentrations and copper isotope ratios in the G93A SOD1 mouse model of amyotrophic lateral sclerosis

Abstract

Amyotrophic lateral sclerosis (ALS) is a motor neuron disease, which involves progressive motor neuron degeneration in the central nervous system (CNS). The G93A SOD1 mouse model simulates one of the most common causes of familial ALS through the overexpression of a mutated form of the human gene encoding copper/zinc superoxide dismutase (SOD1). Transition metals, particularly Cu and Zn, have been shown to behave abnormally in the disease context and have been hypothesized to contribute to and potentially trigger the disease. In this study, concentrations of Cu, Zn and Fe, as well as Cu isotope ratios were assessed in keystone tissues of ALS, including the brain, spinal cord, muscle and whole blood, from transgenic mutant $SOD1^{G93A}$ mice and non-transgenic controls. While no consistent Cu isotope signal was found to be related to the disease state, concentrations of Cu, Zn and Fe were significantly elevated in muscle tissue of the transgenic mice, even at pre-symptomatic time points. In brain and muscle tissue, in both animal groups, a time-dependent Cu isotope signal was observed. We hypothesize that the early and significant elevation in metal concentration in muscle tissue from SOD1 transgenic mice could facilitate the development of ALS, without affecting the overall signal from well-buffered CNS tissues. Ageing may be recorded isotopically as a shift from a neonatal Cu pool as inherited from the mother, through dietary Cu and recycling processes.

Disciplines

Medicine and Health Sciences

Publication Details

Enge, T. Gabriel., Ecroyd, H., Jolley, D. F., Yerbury, J. J. & Dosseto, A. (2017). Longitudinal assessment of metal concentrations and copper isotope ratios in the G93A SOD1 mouse model of amyotrophic lateral sclerosis. Metallomics: integrated biometal science, 9 (2), 161-174.

Longitudinal assessment of metal concentrations and copper isotope ratios in the G93A SOD1 mouse model of amyotrophic lateral sclerosis

T. Gabriel Enge*[1], Heath Ecroyd[2], Dianne F. Jolley[3], Justin J. Yerbury[2] and Anthony Dosseto[1]

Contact: tge571@uowmail.edu.au

Received:

Accepted:

Keywords: Amyotrophic Lateral Sclerosis, ALS, Metals, Copper Isotopes, Medical Isotope Metallomics, G93A, Spinal Cord, Brain, Muscle, Zinc, Iron, Ageing;

Corresponding Author:

T. Gabriel Enge
Wollongong Isotope Geochronology Laboratory
School of Earth and Environmental Sciences
University of Wollongong
Wollongong, NSW, 2522
Australia

[1] Wollongong Isotope Geochronology Laboratory, School of Earth and Environmental Sciences. University of Wollongong, Australia.
[2] Illawarra Health and Medical Research Institute and School of Biological Sciences. University of Wollongong, Australia.
[3] Center for Medical and Molecular Bioscience and School of Chemistry. University of Wollongong, Australia.

Abstract

Amyotrophic lateral sclerosis (ALS) is a motor neuron disease, which involves progressive motor neuron degeneration in the central nervous system (CNS). The G93A SOD1 mouse model simulates one of the most common causes of familial ALS through the overexpression of a mutated form of the human gene encoding copper/zinc superoxide dismutase (SOD1). Transition metals, particularly Cu and Zn, have been shown to behave abnormally in the disease context and have been hypothesized to contribute to and potentially trigger the disease. In this study, concentrations of Cu, Zn and Fe, as well as Cu isotope ratios were assessed in keystone tissues of ALS, including the brain, spinal cord, muscle and whole blood, from transgenic mutant $SOD1^{G93A}$ mice and non-transgenic controls. While no consistent Cu isotope signal was found to be related to the disease state, concentrations of Cu, Zn and Fe were significantly elevated in muscle tissue of the transgenic mice, even at pre-symptomatic time points. In brain and muscle tissue, in both animal groups, a time-dependent Cu isotope signal was observed. We hypothesize that the early and significant elevation in metal concentration in muscle tissue from SOD1 transgenic mice could facilitate the development of ALS, without affecting the overall signal from well-buffered CNS tissues. Ageing may be recorded isotopically as a shift from a neonatal Cu pool as inherited from the mother, through dietary Cu and recycling processes.

Significance to metallomics statement

Copper has been hypothesized to play an important role in the development of amyotrophic lateral sclerosis, an adult onset neurodegenerative disease. Despite knowledge that Cu may contribute significantly, and possibly even trigger the disease phenotype in the central nervous system (CNS), the specific pathways remain obscure. In the present study, we hypothesize that the assessment of transition metal concentrations and Cu isotope ratios in the CNS, muscle and blood can facilitate a better understanding of the ALS aetiology.

Introduction

Amyotrophic lateral sclerosis (ALS) is a fatal neurodegenerative disorder, resulting in the selective death of motor neurons (MNs).[1,2] The degeneration of upper and lower motor neurons causes progressive muscle paralysis and spasticity, affecting mobility, speech, and respiration.[3] Less than 20% of patients survive more than 5 years from diagnosis.[4] Out of all ALS cases, 90-95% are described to be sporadic; the remaining 5-10% familial.[2] These familial cases are predominantly associated with Mendelian-inherited mutations in the genes encoding for Cu,Zn superoxide dismutase (SOD1), TAR-DNA–binding protein 43 (TDP-43), fused in sarcoma/translocated in liposarcoma (FUS/TLS), C9ORF72, and other genes.[4]

The first gene shown to be mutated in familial ALS encodes SOD1[5] and since this discovery, over 150 pathogenic mutations in SOD1 have been identified in ALS patients.[6] While these mutations account for about 20% of the familial cases of ALS[5], the mechanisms behind the selective degeneration of MNs is still unclear; it has been proposed that a variety of pathophysiological processes play a role, including oxidative stress, glutamate-mediated excitotoxicity, protein aggregation and transition metal-induced toxicity.[7] The toxicity induced by mutant SOD1 protein (mSOD1) is proposed to be a toxic gain-of-function rather than a loss of its dismutase activity,[8,9] as a result of increased propensity to destabilize, aggregate and misfold without

proper Zn and Cu coordination. To advance research into ALS, a transgenic mouse model was developed (mutant SOD1-G93A, $SOD1^{G93A}$), in which human SOD1 harboring the G93A mutation is overexpressed (20-24 fold higher expression than endogenous murine SOD1).[8] This mSOD1 mouse model replicates many features of human ALS, including axonal and mitochondrial dysfunction, progressive neuromuscular dysfunction, gliosis and MN loss.[8,10,11] While symptoms become obvious in this mouse model at ~100 days, pathological changes have been observed as early as 30 days of age.[12] Results from experimental data suggest that the binding of Cu and Zn by the mSOD1 may be defective.[13–15]

Transition metals such as Cu, Fe, and Zn, are essential trace elements that function as catalytic cofactors in metalloenzymes (e.g. SOD1 and catalase). At high concentrations, metals can be highly toxic.[16–18] Therefore the concentrations of metals are maintained within a tight concentration range by proteins that mediate their uptake, distribution, storage and excretion.[19,20] A growing body of evidence suggests the involvement of transition metals in the pathogenesis of neurodegenerative disorders, for example Cu and Fe in Parkinson's,[19,21–23] and Cu, Fe and Al in Alzheimer's disease.[24–27] However, the role of Cu and Zn homeostasis in the toxic gain-of-function of mSOD1 associated with the development of ALS remains unresolved.[28]

Current research has not been able to attribute a single metal to be exclusively responsible for MN deterioration in ALS. In the cerebrospinal fluid (CSF) of patients with ALS, significantly elevated concentrations of Mn, Al, Cd, Co, Cu, Zn, Pb, V and U,[29] as well as Mg, Fe, Cu and Zn[30] have been observed, compared to healthy controls, suggesting an accumulation process. However, combinations or synergistic effects between metals may provide explanations to the neurodegeneration in ALS that cannot be attributed to one single metal.[29]

In the G93A mouse model of ALS, the diseased animals have been described to have significantly elevated concentrations of Cu in the spinal cord,[31–35] and this concentration may increase over time with the progression of the disease.[36,37] This increase in Cu concentration was hypothesized to be the result of a mSOD1-dependent shift in intracellular Cu homeostasis toward Cu accumulation in the spinal cord during disease progression: Cu influx increases, Cu chaperones are up-regulated, and Cu efflux decreases.[37] This proposed dysregulation within spinal MNs was proportionally associated with an age-dependent increase in Cu ion concentrations in the spinal cord.[37] When testing the hypothesis that Cu concentrations increase in an age-dependent manner using mice expressing various SOD1 mutants (SOD^{G93A}, $SOD1^{G127X}$, $SOD1^{G85R}$, and $SOD1^{D90A}$), it was found that the amount of Cu bound to the SOD1 active site varied considerably between the mutants. Overall though Cu concentrations were, in every case, significantly increased compared to healthy controls.[32] In another *in vivo* study using mice overexpressing various SOD1 mutants (SOD^{A4V}, $SOD1^{G37R}$, $SOD1^{H80R}$, and $SOD1^{D125H}$), it was found that the SOD1 present in protein aggregates was metal deficient, irrespective of the ability of the mutant SOD1 isoforms to bind Cu.[38] These results suggest a misbalance between the availability and demand for Cu in the cell. In the ventral horn of the spinal cord of the SOD^{G85R} mouse, Fe and Zn are increased in the gray matter, while there is no difference in Cu concentration between white and gray matter.[39] While no significant difference between Cu concentrations in $SOD1^{G93A}$ and non-transgenic littermates

(WT) brain samples were found,[31,36,37,40] a subtle redistribution between the gray and white matter of the spinal cord was observed, with areas of higher Cu concentration correlating to areas of high SOD1 expression, relative to surrounding cells.[40]

In an ALS context, there is currently no consensus concerning Zn concentrations in the spinal cord and brain. When comparing spinal cord concentrations of Zn in tissue from the G93A SOD1 mouse and WT mice, elevated[31,32], depleted[35] and no difference[40] in concentration have been reported. Tokuda et al. (2007)[36] showed that Zn concentrations decreased over time in the spinal cord of diseased mice but remained constant in the brain. Contrastingly, Tokuda et al. (2013)[32] found elevated Zn concentrations in diseased spinal cord tissue compared to transgenic WT animals, which overexpress wild type SOD1 rather than the mSOD1, while the concentrations of Mg, Ca, Al, Mn and Fe were not elevated. Other work indicated a disease-specific increase of Zn in the brain (white matter) of mice expressing mutant SOD1 ($SOD1^{G93A}$, $SOD1^{G37R}$, $SOD1^{H46R}$/$SOD1^{H48Q}$).[40] In a mTDP-43^{A315T} mouse model of frontotemporal lobar degeneration and ALS, elevated concentrations of Zn, Cu and Mn were found in the spinal cord of diseased animals, while concentrations of these metals in the brain remained unaffected.[41]

Iron metabolism has been previously studied in ALS patients, resulting in observations of elevated levels of serum ferritin[42–45] and reduced levels of serum transferrin[43], indicating high overall Fe concentrations in the body. Magnetic resonance imaging of ALS patients indicates abnormal Fe accumulation in the motor cortex,[46–48] which could be responsible for inflammation and oxidative damage. Further findings of elevated Fe concentrations in human CSF[30] and the presence of elevated Fe capable to promote free-radical generation[49] contribute to the hypothesis that a variety of disturbances in Fe metabolism may contribute to the aetiology of ALS.[50]

It has been hypothesized that Cu isotopic ratios in blood and various organs should reflect the efficiency of overall body Cu metabolism,[51–55] but only recently have tools to test this been available. The naturally occurring stable isotopes of Cu ($^{65}Cu/^{63}Cu$) are expected to distribute as a function of coordination and bond energy. Heavy isotopes are anticipated to be enriched in the strongest bonds, since the vibrational energy decreases at higher isotope mass.[56,57] Hence, at the cellular level, it is likely that the Cu isotopic ratio is influenced by Cu-specific cell ligands.[58,59]

Recent research has seen the application of medical isotope metallomics to a wide variety of medical problems.[56,60] Important pilot studies were able to demonstrate the potential of medical isotope metallomics as a medical diagnostic tool: bone loss was traced via changes in Ca isotope ratios in blood and urine,[61,62] cancer disease progression was traced via Cu and S isotopes in blood plasma,[59,63] a correlation between liver cirrhosis severity and blood serum Cu isotope ratios was discovered[64] and breast cancer cells identified via Zn isotopes.[65,66] The methodology was also applied to Parkinson's disease, a neurodegenerative disease, where it was shown that patients appear to have abnormalities in their Cu metabolism.[22]

The potential of medical isotope metallomics as a diagnostic tool has been reviewed for a variety of conditions.[67] In this study it was tested whether there is a detectable longitudinal ALS-signal in metal (Cu, Zn, Fe) concentrations and Cu isotope ratios in

keystone tissues (brain, spinal cord, muscle tissue and whole blood) involved in the pathogenesis of ALS in the $SOD1^{G93A}$ mouse model. These longitudinal results were collected to improve our understanding of the involvement of transition metals in the development of ALS and the potential for Cu isotopes to serve as a prognostic/diagnostic tool for the disease.

Samples

Transgenic mice in this study expressed the G93A mutant form of human SOD1 (B6SJL-Tg(SOD1*G93A)1Gur/J)[8] (Jackson Laboratory, ME, USA), from here on referred to as '$SOD1^{G93A}$'. Healthy controls were non-transgenic littermates (WT). The mice were bred under specific conditions in accordance with Australian animal ethics laws at Australian Bioresources (Mossvale, NSW). The University of Wollongong animal ethics committee approved all experimental procedures (Ethics Number: AE14/28). All animals had free access to a uniform diet and water, and were held on a regulated 12 hours day-night light cycle. Mice were euthanized by CO_2 asphyxiation, immediately dissected to collect blood and various tissue samples, which were snap frozen in liquid nitrogen. All mice were female to avoid gender differences in the data. Mice were 30, 60, 90 or 120 days old (±2 days) to capture the characteristic disease progression typical for this mouse model.[68] Samples of the uniform mouse food diet were randomly collected from various locations at the breeding facility (Australian Bioresources). Samples of DORM-2 dogfish muscle, certified reference material of the National Research Council Canada (CRM, NRCC), were used to test the completeness of the sample digestion protocol.

Analytical techniques

Sample digestion

Mouse tissues, food and DORM-2 (~0.25 g) were weighed, and pre-digested in MARSXpress 20 mL PFA vessels in 2.5:1 mixture of 15 M Ultrapur® HNO_3 (Merck) and Ultrapur® 30% H_2O_2 (Merck) for 30 minutes. These samples were further digested using a MARS6 (CEM Corporation, North Carolina, USA) microwave system at the University of Technology, Sydney. Temperature was ramped to 210 ºC over 15 min and then held constant for 150 min to ensure that all organic carbon was oxidized to $CO_{2(g)}$. For quality control purposes, one blank (acid only) and two DORM-2 aliquots were added to each digestion batch. Recovery of elements (Cu, Fe, Zn) from the DORM-2 certified reference material was used to control that the digestion of the biological samples was complete (Table 1).

Table 1 – Recoveries of select metals from DORM-2 (CRM, NRCC), in mg kg^{-1} (n=12)

Element	Certified Value	2SD	Measured Value	2SD	Recovery (%)
Cu	2.34	0.16	2.4	0.3	103
Fe	142	10	147	55	104
Zn	25.6	2.3	28	8	109

Elemental Concentrations

Copper, Fe and Zn concentrations were determined using a Thermo Scientific iCAP-Q quadrupole-inductively coupled plasma-mass spectrometer (Q-ICP-MS) at the Wollongong Isotope Geochronology Laboratory, University of Wollongong (WIGL, UOW). The concentrations were quantified using a multi-element standard external calibration curve; long-term instrument drift was corrected using a 50 ppb Ga solution as internal standard. Accuracy of the measurements were assessed through the

analysis of the DORM-2 CRM which yielded recoveries of 103% for Cu, 104% for Fe and 109% for Zn (Table 1). Reproducibility assessed through the analysis of DORM-2 samples with every digestion batch was 12% for Cu, 30% for Zn and 55% for Fe (2RSTD). Total procedure blanks were assessed as <2 ng Cu, <4 ng Fe and <10 ng Zn.

Copper Isotopic Measurement

Copper was purified via ion exchange chromatography following the protocol described previously[69] in a cleanroom (WIGL, UOW). The Cu eluates were evaporated to dryness and refluxed in 0.3 M HNO_3. Stable Cu isotope analysis was performed via multi collector-inductively coupled plasma-mass spectrometer (MC-ICP-MS), using a Neptune Plus (Thermo Scientific) at WIGL, UOW. Standard sample and skimmer cones, cyclonic spray chamber and PFA nebulizer with ~100 µL min^{-1} flow rate (Elemental Scientific, Omaha, USA) were used throughout. Routine instrument sensitivities of 20 V ppm^{-1} were achieved. The measurements were corrected for instrumental mass fractionation through a combination of internal correction with admixed Ni[70] and applying Russell's exponential law[71]. External normalization was achieved using a standard sample bracketing approach with the Cu isotopic reference material ERM-AE633 (European Commission, Geel, Belgium), as described previously elsewhere.[72,73] Typical measurement accuracy of a synthetic standard solution ($Cu_{SRM-976}$, National Institute of Standards and Technology, Bethesda, MD, USA) was better than 0.01‰ (2SE; n = 197). Due to the lack of a certified biological isotopic reference material, the long-term measurement reproducibility and accuracy was tested on repeat measurements of food sample aliquots: $\delta^{65}Cu$ = 0.84 ± 0.03‰ (2SE, n=6). Therefore the external error for the isotopic measurements is defined as 0.03‰ (2SE). The isotopic composition of Cu is expressed using the delta notation ($\delta^{65}Cu$, ‰) (Eqn. 1). Total procedure blanks were assessed to be <2 ng of Cu, therefore negligible compared to the usual 200-400 ng of Cu found in the tissue samples.

$$\delta^{65}Cu = \left[\frac{(^{65}Cu/^{63}Cu)_{\text{Sample}}}{(^{65}Cu/^{63}Cu)_{\text{ERM-AE633}}} - 1 \right] \times 1000 \qquad (1)$$

Statistical Methods

In order to assess the results from the measured data set, statistical analysis was performed. All statistical analyses were conducted using the statistical program R v3.3.1.[74] Prior to analysis, outliers were removed using the median average deviation (3*mad). Any measurements outside 3*mad were considered to be measurement artifacts or the result of contamination. Data were analyzed through a linear regression model for each organ type with disease state and time used as independent variables and the measurements of Cu, Fe and Zn, as well as Cu isotope ratios, as dependent variables. Time was treated as a continuous variable. Likelihood ratio tests[75] were used to determine which independent variables were significant. The assumptions of the linear regression model were checked, including normality tests for residuals. A significance level of $\alpha = 0.05$ was used.

Results

Metal concentrations

Spinal cord

In spinal cord tissues, Cu, Zn and Fe concentrations do not vary considerably between SOD1^{G93A} and WT samples (Table 2, 3 and Fig. 1A). Temporal behaviors of all three metals are similar in that they increase until 90 d and then decrease, with the exception of Zn in the SOD1^{G93A} tissue, where concentrations keep increasing until 120 d (Fig. 1A-C). Zinc concentrations further show unexpectedly high values and large variability at 90 d.

Brain

Similarly to the spinal cord tissues, brain tissues also do not display a significant variation between SOD1^{G93A} and WT tissues for any of the assessed metals (Tables 2 and 3). All three metals show similar trends with age, in both SOD1^{G93A} and WT, where concentrations increase until 60 or 90 d and then decrease. These trends appear to be more pronounced in Cu and Fe (Table 2 and Fig. 1D-F), but only reach statistical significance for Cu ($p = 0.004$).

Muscle

Different to the other tissues, concentrations in muscle tissue do vary significantly between SOD1^{G93A} and WT mice: Cu ($p < 0.0005$), Zn ($p < 0.0005$) and Fe ($p = 0.004$) (Table 2, 3 and Fig. 1G-I). The difference between the concentrations in SOD1^{G93A} and WT mice appears to be a pre-symptomatic feature in Cu and trailing the development of symptoms (i.e. 60 d) in Zn and Fe (Fig. 1G-I). The concentrations of all three metals increase until 90 d in the SOD1 tissue and then slightly decrease. In WT mice Cu, Zn and Fe concentrations are relatively constant over time (Fig. 1G-I), while the concentrations of Zn show a larger variability at 60 d.

Whole Blood

In whole blood, none of the analyzed metals vary significantly between SOD1^{G93A} and WT mice (Table 2, Fig. 2). Iron concentrations demonstrated a significant trend over time ($p = 0.05$), where concentrations from both populations decrease between 30-60 d and then increase until 120 d (Fig. 2C).

Table 2 – Metal concentrations and Cu isotope ratios for spinal cord, brain and muscle tissues, and whole blood.*

	State	n	30 d	n	60d	n	90d	n	120 d
Spinal cord									
Cu (μg g^{-1})	SOD1^{G93A}	6	9 ± 7	6	21 ± 12	5	19 ± 12	6	16 ± 14
	WT	7	12 ± 12	6	15 ± 10	6	18 ± 8	6	12 ± 11
Zn (μg g^{-1})	SOD1^{G93A}	6	52 ± 28	6	83 ± 49	5	87 ± 60	6	89 ± 65
	WT	7	56 ± 43	6	53 ± 31	6	97 ± 59	5	45 ± 46
Fe (μg g^{-1})	SOD1^{G93A}	6	56 ± 55	6	100 ± 80	5	104 ± 72	6	95 ± 69
	WT	7	90 ± 110	6	80 ± 54	6	109 ± 58	5	64 ± 21
δ^{65}Cu (‰)	SOD1^{G93A}	6	1.7 ± 0.8	6	1.4 ± 1.1	6	1.7 ± 1.2	6	1.6 ± 0.7
	WT	7	1.7 ± 0.7	6	2.1 ± 0.7	6	1.2 ± 0.6	6	1.5 ± 1.1
Brain									
Cu (μg g^{-1})	SOD1^{G93A}	6	14 ± 2	6	27 ± 13	5	29 ± 14	6	25 ± 7
	WT	7	16 ± 6	6	28 ± 12	6	27 ± 19	6	23 ± 3
Zn (μg g^{-1})	SOD1^{G93A}	6	87 ± 40	6	121 ± 50	5	94 ± 98	6	97 ± 38
	WT	7	76 ± 47	6	110 ± 45	6	108 ± 80	6	78 ± 18
Fe (μg g^{-1})	SOD1^{G93A}	6	73 ± 18	6	122 ± 34	6	110 ± 120	6	94 ± 39
	WT	7	80 ± 25	6	128 ± 46	6	120 ± 84	6	102 ± 24
δ^{65}Cu (‰)	SOD1^{G93A}	6	1.8 ± 0.4	6	1.3 ± 0.8	6	1.5 ± 0.4	6	1.3 ± 0.4

	WT	7	1.8 ± 0.8	6	1.6 ± 0.8	6	0.9 ± 2.2	6	1.4 ± 0.8
Muscle									
Cu (μg g^{-1})	SOD1^{G93A}	6	7 ± 5	6	17 ± 8	6	24 ± 15	6	13 ± 5
	WT	6	5 ± 4	6	7 ± 5	5	6 ± 3	6	4 ± 1
Zn (μg g^{-1})	SOD1^{G93A}	6	48 ± 20	6	97 ± 64	5	117 ± 63	6	95 ± 47
	WT	6	42 ± 19	6	68 ± 56	5	49 ± 24	6	37 ± 14
Fe (μg g^{-1})	SOD1^{G93A}	6	47 ± 18	6	74 ± 26	5	146 ± 23	6	120 ± 96
	WT	6	50 ± 26	6	74 ± 42	5	65 ± 37	6	47 ± 6
δ^{65}Cu (‰)	SOD1^{G93A}	6	2.2 ± 1.8	6	1.0 ± 2.0	6	0.7 ± 0.9	6	0.5 ± 1.3
	WT	6	2.0 ± 1.6	6	1.7 ± 1.9	6	1.1 ± 2.2	6	0.7 ± 0.6
Blood									
Cu (μg g^{-1})	SOD1^{G93A}	6	5 ± 3	7	3 ± 3	7	3 ± 4	8	4 ± 3
	WT	8	4 ± 2	8	3 ± 3	7	3 ± 4	8	3 ± 1
Zn (μg g^{-1})	SOD1^{G93A}	7	25 ± 10	7	31 ± 21	7	35 ± 27	8	33 ± 19
	WT	9	23 ± 14	8	31 ± 27	7	34 ± 24	8	26 ± 7
Fe (μg g^{-1})	SOD1^{G93A}	7	2100 ± 1800	7	1700 ± 1900	7	1600 ± 2500	8	2900 ± 1700
	WT	9	2200 ± 1700	8	1800 ± 2300	8	1800 ± 2700	8	3000 ± 500
δ^{65}Cu (‰)	SOD1^{G93A}	7	1.1 ± 0.7	8	0.7 ± 1.7	8	0.8 ± 1.2	8	1.3 ± 1.2
	WT	9	1.1 ± 0.8	8	0.9 ± 1.0	8	0.6 ± 0.9	8	1.2 ± 1.3

*Concentrations (μg g^{-1}) are presented for the diseased (SOD1^{G93A}) and healthy, non-transgenic (WT) samples against time (in days; d). Errors shown are 2 standard deviations of the repeat measurements.

Table 3 – Maximum and minimum metal concentrations and Cu isotope ratios for spinal cord, brain and muscle tissues, and whole blood.

	SOD1^{G93A}		**WT**	
Spinal cord	min	max	min	max
Cu (μg g^{-1})	4	24	4	24
Zn (μg g^{-1})	27	122	20	142
Fe (μg g^{-1})	35	183	46	195
δ^{65}Cu (‰)	0.8	2.4	0.8	2.5
Brain				
Cu (μg g^{-1})	13	38	9	38
Zn (μg g^{-1})	15	140	34	156
Fe (μg g^{-1})	18	216	41	169
δ^{65}Cu (‰)	0.9	2.2	-1.3	2.2
Muscle				
Cu (μg g^{-1})	4	39	3	11
Zn (μg g^{-1})	15	140	34	156
Fe (μg g^{-1})	37	205	38	102
δ^{65}Cu (‰)	-0.2	3.9	0.4	3.3
Blood				
Cu (μg g^{-1})	1	8	1	6
Zn (μg g^{-1})	18	60	16	53
Fe (μg g^{-1})	51	4008	48	4166
δ^{65}Cu (‰)	-0.3	2.4	-0.1	2.2
Feces				
Cu (μg g^{-1})	36	104	50	115
Zn (μg g^{-1})	257	442	273	835
Fe (μg g^{-1})	1011	2771	1099	1781
δ^{65}Cu (‰)	0.6	1.9	0.5	1.4

Food and Feces

Mouse food samples show Cu, Zn and Fe concentrations of 13.7 ± 0.5, 76 ± 5 and 340 ± 30 μg g-1, respectively (2SE, n = 6). In feces, there is no significant difference in metal concentrations between SOD1^{G93A} and WT samples, and no trends over the age of the mice (Table 3 and 4).

Copper isotope ratios

Spinal cord

In the spinal cord, Cu isotope ratios vary between 0.83 and 2.44‰ for SOD1^{G93A} mice, and between 0.65 and 2.46‰ for WT mice (Fig. 3A, Table 3), with the difference only being significant at 60 d ($p = 0.0328$) as a result of unusually positive Cu isotope ratios in the WT tissue. Over time, no systematic variation was observed in either population.

Brain

In brain tissue, the Cu isotope ratios vary between 0.9 and 2.2‰ for SOD1^{G93A}, and between -1.3 to 2.2‰ for WT mice (Fig. 3B, Table 3) with the difference not reaching statistical significance. Across time, in both groups the isotope ratios decrease from 1.8‰ at 30 d, to 1.3-1.4‰ at 120 d (Table 2; $p = 0.011$).

Muscle

In muscle tissue, the Cu isotope composition varies between -0.2 and 2.4‰ for SOD1^{G93A} mice, and between -0.4 to 3.3‰ for WT animals (Fig. 3C). Similar to the trends observed in brain tissue, the isotope ratios decrease between 30-120 d, but this trend is more pronounced, from ~2‰ at 30 d to 0.5-0.7‰ at 120 d (Table 2; $p < 0.0005$).

Whole Blood

In whole blood the Cu isotope ratios vary between 0.6 and 1.9‰ for SOD1^{G93A}, and between 0.5 and 1.4‰ for WT mice. These Cu isotope ratios fluctuate around 0.83‰, which is the isotope ratio of food (Fig. 4A). Overall there is no significant difference between SOD1^{G93A} and WT mice.

Food and Feces

Mouse food samples have a Cu isotope ratio of 0.84 ± 0.03‰ (2SE, n=5), which is at the lower end of the observed values and similar to those observed in blood (Fig. 4A). The average Cu isotope ratio of all mouse feces samples is also 0.84 ± 0.59‰ (2SD, n=24), while SOD1^{G93A} mouse feces average at 0.92 ± 0.66‰ (2SD, n=12) and WT mouse feces at 0.77 ± 0.48‰ (2SD, n=12) (Fig. 4B). There is no significant difference between the two populations or changes with time (Table 4).

Table 4 – Metal concentrations (Cu, Fe, Zn) (µg g^{-1} ± 2SD) and Cu isotope ratio (‰ ± 2SD) in mouse feces

time	*State*	*δ^{65}Cu*	*Cu*	*Fe*	*Zn*	*n*
30	SOD1^{G93A}	0.89 ± 0.42	53 ± 34	1210 ± 540	350 ± 170	3
	WT	0.67 ± 0.09	57 ±10	1270 ± 310	357 ± 8	3
60	SOD1^{G93A}	0.85 ± 0.29	85 ± 33	1470 ± 160	400 ± 51	3
	WT	0.94 ± 0.87	60 ± 21	1280 ± 210	320 ± 85	3
90	SOD1^{G93A}	1.19 ± 1.16	88 ± 18	1600 ± 530	410 ± 62	3
	WT	0.66 ± 0.33	90 ± 51	1600 ± 400	450 ± 33	3
120	SOD1^{G93A}	0.73 ± 0.35	90 ± 39	2000 ± 1500	400 ± 76	3
	WT	0.77 ± 0.24	61 ± 11	1620 ± 230	500 ± 570	3

Discussion

Accumulation of metals

It has been previously hypothesized that changes in Cu and Zn concentrations play an important role in the gain-of-toxic function associated with mSOD1.[76,77] This has

been supported by findings that (1) Cu chelators, such as *D*-penicillamine and Trientine, can prolong survival of SOD1^{G93A} mice,[78,79] by reducing the overall available Cu, (2) the ATPase ATP7B, a Cu transporter, is down regulated in the spinal cord of SOD1 transgenic mice (G93A),[68] (3) delivery of Cu via the blood-brain-barrier permeable complex Diacetylbis(N(4)-methylthiosemicarbazonato) Copper(II) (Cu^{II}(atsm)) to Cu-deficient SOD1 converted it to stable holo-SOD1 in the SOD1^{G37R} mouse model, prolonging survival,[28] suggesting a therapeutic target for increased Cu concentrations, and (4) Zn deficient mSOD1 can induce motor neuron apoptosis via peroxynitrite-mediated tyrosine nitration.[80] Apart from these findings, Cu and Zn have an antagonistic interaction,[81] meaning that dyshomeostasis of one could prevent the proper utilization of the other.[32] Overexpression of mSOD1 (e.g. the SOD1^{G93A} mouse model of ALS used in this work) was proposed to lead to increased Cu concentrations in spinal cord tissue, due to a proposed increased affinity of mSOD1 for Cu, making it an effective Cu sink.[82] However, a recent review[77] concluded that partially metalated intermediate SOD1 species may account for the observed SOD1 toxic-gain of function. Taking this into account with an overall increased concentration of the mSOD1 in the SOD1^{G93A} model, Cu concentrations in ALS affected tissues are therefore expected to increase, compared to healthy controls.

Spinal cord

Overall, all metals (Cu, Zn, Fe), show a similar behavior: after a marked increase of Cu concentration from 30-60 d, the concentrations peak at 90 d, and decrease towards 120 d, without significant differences between healthy and diseased tissues (Fig. 1A-C). Lelie *et al.*[40] found a redistribution of Cu between the gray and white spinal cord matter of SOD1^{G93A} mice, which may not be reflected in bulk analyses as performed in this study. Zinc concentrations are an exception as in the SOD1^{G93A} mouse they were found to keep increasing until 120 d. Furthermore, the WT tissue shows a marked rise from 60-90 d with unexpected high concentration of Zn at 90 d and then a decrease at 120 d. Recent findings[83] suggest that the interaction between the Cu chaperone (CCS) and SOD1 is perturbed, such that, during the metalation and maturation of SOD1, the Zn atom is not incorporated properly into its structure. This would negatively impact disulphide formation and Cu activation of SOD1.

Previous work[32–37,41] has found significantly elevated Cu concentrations in spinal cord tissue of several mouse models of ALS, which was suggested to be the result of mSOD1 in the SOD1^{G93A} mouse having a higher affinity to bind Cu ions, leading to increased Cu in spinal cord tissue compared to WT mice.[37] However, recent work[84] did not find a significant difference between non transgenic WT and SOD1^{G37R} spinal cord tissue, similar to findings presented here (Fig. 1A). The previous observations of increased Cu concentrations, particularly in mouse models of ALS that involve over-expression of SOD1, may therefore be reflective of the increased amount of SOD1 expressed in these mice. It is further possible that this signal indicates the presence of free, but not bio-available, Cu, rather than a side effect of an increased binding affinity,[82] as previously proposed. A recent review highlighted the increasing evidence for the involvement of partially metalated SOD1 in ALS development,[77] which is supported by work with SOD1^{G37R} mice whereby Cu was delivered directly to spinal cord mSOD1 via Cu^{II}(atsm).[28,85] This direct delivery decreased the amount of metal deficient SOD1, while it improved the amount of fully metalated-SOD1 present,[28] as well as the phenotype of ALS. Previous work has found mixed results of reduced Zn concentrations,[35,36] no difference[40] and increased concentrations,[31,32,84] in

various mSOD1 mouse model compared to controls. A lack of variation in Fe concentrations in the spinal cord in SOD1^{G93A} and WT over time and against one another is in agreement with prior findings.[31]

Brain

The SOD1^{G93A} and WT tissues had similar trends in all three metals, without there being a significant difference between the animal groups (Fig. 1D-F). A dramatic increase from 30 to 60 d, was followed by a slow decrease in Cu, Zn and Fe. The lack of difference between the SOD1^{G93A} and WT tissues suggests that these trends may be the result of ageing, which is only significant for Cu concentrations. While higher concentrations of Cu and Zn in brain tissue were previously found in the SOD1^{G37R} mouse model,[84] our findings are in accordance with other work using mSOD1 mouse models (G37R, G93A, H46R/H48Q), where no differences were observed.[31,36,40] This lack of increased concentrations, could be the result of a lack of an ALS-related up-regulation of Cu trafficking to the cerebellum,[37] and that only a small area of the brain is affected which may be difficult to detect when measuring the metal concentration in the whole brain.

Muscle

Muscle tissue from diseased mice consistently demonstrated higher metal concentrations than WT samples in accordance with previous findings,[84] with increases in Cu and Zn concentrations preceding the establishment of symptoms (Fig. 1G-H) and Fe trailing them (Fig. 1I). Skeletal muscle is one of the largest organs in the human body, comprising ~40% of the whole body lean mass; muscles and bones together contain ~50% of total body Cu.[86] Muscle tissue provides a source for amino acids during stress and forms a crucial part of whole body metabolism and homeostasis,[87] while also being suggested to contain a surplus of SOD.[88] In ALS, muscle tissue,[89–91] and other (neighboring) cell types[92] may play a significant role in pathology development. Distinct and rapid muscle atrophy caused by MN death is a pathologic hallmark of ALS.

The accumulation of excess Cu and Zn in muscle observed in this study could be the consequence of the over expression of the mSOD1 protein in the SOD1^{G93A} mouse, whereby the increased concentrations reflect an increased requirement for Cu and Zn by the partially metalated protein, similar to previous findings in the SOD1^{G37R} mouse model[84]. However, if the increases are not a consequence of the over-expression of SOD1 in this mouse model, they may indicate a causal pathologic feature of ALS, whereby accumulation of Cu and Zn in muscle could be toxic, resulting in MN death. This would support the dying-back-hypothesis[93]: ALS may be a dying back motor neuropathy whereby distal axonal degeneration occurs and this precedes neuronal degeneration.[94,95] The axon and neuromuscular junction are affected at an earlier stage prior to the onset of symptoms and neurodegeneration, which may indicate that intrinsic defects in the muscle occur early, promoting or contributing to withdrawal of the motor axon.[96] Signaling between the muscle and the neuron is important for axonal growth and management of the neuromuscular junction,[97] while the loss of signal from the neuron to the muscle leads to atrophy. It is also possible that muscle defects may be independent of axonal withdrawal,[96] leading to the assumption that skeletal muscle is likely to be one of the primary targets of ALS-associated mutations. While the origin of the here-observed accumulating metals remains unknown, Cu isotope analyses (see below) suggest that the Cu could originate from a dietary,

exogenic Cu source, however, the direction of and magnitude of changes (increase of influx vs decrease of efflux vs changes to recycling processes) are unclear.

Whole blood

There were no significant trends in metal concentrations of Cu and Zn in whole blood over time or between the SOD1^{G93A} and WT samples. Iron concentrations are an exception, as they follow a trend over time such that the concentration decreases between 30-60 d and then increases until 120 d (Fig. 2A-C). Mixed results have been documented for Cu concentrations in blood serum and ceruloplasmin: concentrations have been reported to be decreased in ALS patients, compared to healthy controls,[98,99] or to not be significantly different[100], similar to the here presented data. This may be a side effect of the short residence time of these metals in blood (e.g. 7-14 d for Cu in mice[101]), robust excretion mechanisms,[101] and low Cu concentration compared to humans.[101,102] These may therefore account for the lack of positive association with disease progression. One study on human blood reported a positive association between Cu concentrations and ALS, while Zn was inversely associated.[103]

Feces

Feces samples did not demonstrate a difference between SOD1^{G93A} and WT samples, for any of the assessed metals. For Fe and Cu, a time dependent increase in concentration was found, which is most likely the result of the higher dietary requirement of the larger mice. Overall, no disease dependent anomalies of metal uptake or excretion were detected.

Copper isotope ALS signal

The Cu isotopes display a scattered pattern for spinal cord tissue without any clear trends (Fig. 3A). Brain (Fig. 3B) and muscle tissue (Fig. 3C) follow a similar time-dependent trend, whereby isotope ratios start at a more positive value at 30 d and then shift towards less positive values. The same trend was observed in SOD1^{G93A} and WT tissues. In blood (Fig. 4A), no significant difference was detected between SOD1^{G93A} and WT. It was observed, however, that the blood and feces isotope ratios (Fig. 4) fluctuate around 0.84‰, i.e. the value of food, indicating that the isotope signal is more a reflection of the diet than the disease. Overall, the isotope ratios from tissues from the SOD1^{G93A} mouse model of ALS presented here indicate that there is no presence of a clear ALS-associated Cu isotope signal.

It has been postulated that stable isotope ratios can inform about past oxidation conditions in geological and biological systems.[104] Isotope ratios of Cu[59,63,105] and Zn[65,66] change in association with cancer development and Cu isotope ratios with liver cirrhosis.[64] In the example of cancer, hypoxic (reducing) conditions within the tumor's environment can impair the metabolism of Cu and change the metal's redox state. This is the consequence of the binding ability of specific molecules, inducing isotopic fractionation, which is measurable.[59]

A variety of neurodegenerative diseases have been associated with excessive oxidative stress[106–110] including ALS where oxidative stress has been identified to be of great importance,[111] in both humans and rodent models.[112] Two mechanisms have been identified to induce oxidative stress in cells in relation to Cu: (1) a Fenton-like reaction that can directly catalyze reactive oxygen species (ROS) generation,[113] (2) exposure to elevated concentrations of Cu, which significantly decreases the levels of

glutathione (GSH).[114,115] A decrease in GSH limits the cell's antioxidant ability, contributing to shifting the redox balance towards more oxidizing conditions.[18,88] This may also enhance the cytotoxicity of ROS and allow Cu to be more catalytically active, resulting in the production of even more ROS.[116] In ALS, mitochondrial dysfunction was reportedly responsible for increases in the free radical generation,[109,117,118] followed by oxidative stress and associated calcium toxicity following glutamate receptor activation.[118] As a result, it was expected that there should be a direct correlation between disease progression and the development of oxidative stress,[119,120] leading to Cu isotope fractionation, and an ALS-associated Cu isotope signal.

The observed lack of a Cu isotope signal in the SOD1^{G93A} mouse model of ALS may be the result of several factors. First, ROS production does increase as a function of time (ageing-effect) in SOD1 transgenic mice,[121] which would require ROS to be relatively more increased to be able to be traced as a deviation of the signal that arises from ageing alone. Second, in the spinal cord of the SOD1^{G93A} mice two metallothionein-I/II (MT-I/II) isoforms were previously found to be significantly elevated, which act as Cu chaperones, sequestering free Cu[122] as a compensatory reaction to Cu-mediated oxidative stress, even at pre-symptomatic stages.[36] It was later found that overexpression of MT-I in the SOD1^{G93A} mouse model prolongs survival and restores Cu dyshomeostasis,[33] which suggests that ROS production could be regulated and a resulting Cu isotope signal dampened.

Finally, it is widely accepted that it is not the loss of antioxidant function of mSOD1 that leads to the development of pathology, but rather a separate toxic gain-of-function.[9] While this toxic gain-of-function was confirmed by transgenic mice overexpressing mSOD1, where the level of mSOD1-expression was proportional to the onset and severity of symptoms,[8,123,124] it has proved difficult to elucidate the specific mechanisms of mSOD1 toxicity.[77] Given that the ALS-like phenotype of the SOD1^{G93A} mice used in this study is driven by the expression of the mSOD1 and to a lesser extend its over expression, it is reasonable to assume that the inferred oxidative stress would not be reflected in a changed isotope signature in the target tissues. When taking into account that in brain and spinal cord tissue there is little to no difference in Cu concentrations between SOD1^{G93A} and WT tissue (Fig. 1A, D), this suggests that, in addition to the tight control of Cu influx through the blood-brain-barrier,[88,125] the binding of Cu to various proteins/binding sites not does alter as a result of the disease. The alteration may further be too subtle to be detected using stable isotope techniques at the currently available resolution. Changes in Cu concentration in tissues may be attributable to the overall higher concentration of mSOD1 in the transgenic mice or the up-regulation of cupro-proteins as a side effect of mSOD1 overexpression, possibly leading to cell specific deficiencies of Cu, resulting in no change to the isotope ratio in the tissue.

The significantly elevated Cu concentrations in SOD1^{G93A} muscle tissue (Fig. 1G) offer a slightly different picture: muscle tissue, compared to central nervous system tissues, is subject to less stringent regulation of Cu transport.[88] Muscle tissue in general was noted to be a major repository of metals, and contains a surplus of SOD1.[88] A tracer study using ^{64}Cu observed that young (neonates, 10-12 d) mice retained significantly more Cu than adult counterparts in muscle tissue.[126] We hypothesize that muscle tissue may, at least in part, serve as a reservoir for exogenic,

dietary Cu, and its natural Cu isotope signature may, therefore, alter to become more similar to that of the food source over time (30 – 90 d) (Fig. 3C). Further to the assimilation, it is plausible to assume that recycling processes can further enhance the preferential uptake and retention of the lighter Cu isotope over time, indicating that Cu may accumulate in the weaker bonds[56,57]. While there is overall more Cu in the $SOD1^{G93A}$ muscle tissue (Fig. 1D), it binds to the same protein binding sites as in the WT controls. This is supported by the Cu isotope ratios measured in this work (Fig. 3C) whereby the ratios move in the same direction in $SOD1^{G93A}$ and WT mice. However, $SOD1^{G93A}$ tissue appears to follow a steeper decline towards the isotope ratio of food (0.84‰), suggesting that cupro-proteins, using weaker bonds, may be up-regulated and accumulate Cu, as previously suggested for several other tissues.[29,37] This accumulation of Cu could then lead to a dying backward process, in the form of a distal motor neuropathy.[1,127]

Cu isotope ageing signal

The Cu isotope ratios for muscle and brain tissue in this study demonstrate a similar age-dependent trend, which is independent of disease state. The Cu isotope compositions are positive at 30 d (~2‰) and then decrease over time (Fig. 3B and C). It is well known that organisms accumulate certain metals in various tissues and fluids over the course of their lifespan.[19,128,129] As the oldest mice tested in this study were 120 d old (still comparatively young, equivalent to ≈ 20-30 y in humans[130]), it is surprising that a Cu isotope ageing-signal may already be present. The downward trends are more pronounced in muscle than in the brain, which could be a result of the different rates of metabolism in these different organs, as observed in humans, where female breast tissue ages faster than other organs.[131] A precise assessment of ageing in individual organs remains difficult.

In order to determine whether the signal observed here is indicative of ageing, it is important to control for any potential age-related changes in Cu absorption that may affect the signal. In men and women between 20 and 83 y, there is no significant change in Cu absorption over time[132] and Cu absorption is tightly regulated as a function of available dietary Cu.[133] As the mice used in this study (and their parents before them) were given a uniform and standardized diet, it is reasonable to assume that trends over time are a true expression of ageing, rather than the result of variability in diet with age.

It is well known that during mammal pregnancy, metals (nutrients) are transported from the mother across the placenta to the fetus, where they cross the fetal endothelium and enter circulation (Fig. 5).[134] These metals (e.g. Fe and Cu) are then stored in the fetal liver and are rapidly liberated to facilitate growth after birth.[88,135,136] Copper transport to the fetus increases in the last trimester and is chaperone specific.[137] The Cu accumulates in the placenta in the form of ceruloplasmin, $CuHis_2$, or other low molecular complexes.[138] In absence of ceruloplasmin, Cu transport is not inhibited, highlighting the potential importance of the $CuHis_2$ pathway in the transport.[134] Based on *ab initio* calculations, histidine containing compounds, such as ceruloplasmin and $CuHis_2$ [$Cu^{2+}(His)_2$] have previously been hypothesized to concentrate the heavier isotope of Cu.[58] In this study, more positive Cu isotope ratios (accumulation of heavier isotopes) in brain and muscle samples (Fig. 3B and C) were found at 30 d. These results suggest the presence of a 'starting pool' of 'heavy' Cu received from the mother, which is then diluted, recycled or changed over time

through exogenic, dietary Cu and endogenic metabolic Cu recycling processes (Fig. 6).[88,139,140]

Conclusion

The assessment of metal concentrations in tissues from healthy and ALS mice yielded contrasting results. Brain and blood samples showed no definitive trends between diseased and healthy tissues, while Zn concentrations in spinal cord and muscle tissue, and Cu concentrations in muscle tissue were elevated at pre-symptomatic stages in the diseased tissues. An increase in Fe concentrations in muscle trailed the development of symptoms. Observed pre-symptomatic changes in metal concentrations in the results from muscle tissue may support the dying-back hypothesis as a function of toxicity induced by the accumulation. This warrants further investigation into the potential applicability of metal concentrations as biomarkers for ALS. Copper isotope ratios revealed no clear disease-based signal in any of the tissues. When considering the higher Cu concentrations and changes in isotope ratios in the SOD1 mouse muscle, it could suggest that either the association of Cu with specific binding sites does not change or that possible changes in the association of Cu with other binding sites is below the detection limit of the applied method. Future studies should consider overcoming the limitations of the mSOD1 over expression models by using transgenic mice, which over express wild type SOD1. This way effects induced by the increased expression of SOD1 can be accounted for.

In muscle and brain tissue, changes in isotope composition over time were observed, suggesting the presence of an ageing signal. This potentially presents a new way of looking at the concept of metabolic ageing, whereby the speed of ageing can be determined by turn-over rates of recycling and accumulation processes of Cu in certain tissues, as a deviation from the fetal Cu pool. Mice currently present one of the best model organisms to study ALS and ageing. A promising direction for future studies is the application of metal concentration and Cu isotope measurements to human samples, including blood plasma and potential muscle biopsies, and to specific cell types, to understand the involvement of Cu and other metals in the aetiology of ALS.

Acknowledgements

The authors want to thank Michael Ellwood (Research School of Earth Sciences, the Australian National University) for providing a NIST-976 solution. Luke McAlary is thanked for useful discussion, Andrew Zammit Mangion for guidance in the data pre-processing and James P. Dawber with the statistical analysis. Philip Doble and the University of Technology, Sydney granted TGE visitor status to perform some of the microwave digestion work at their facilities. This work was funded by Australian Research Council Discovery grant DP140100354 and a SMAH Small Project grant. TGE acknowledges a Discovery University Postgraduate Award.

References:

1 R. L. Redler and N. V Dokholyan, *Prog. Mol. Biol. Transl. Sci.*, 2012, **107**, 215–62.

2 L. P. Rowland and N. A. Shneider, *N. Engl. J. Med.*, 2001, **344**, 1688–1700.

3 O. Hardiman, L. H. van den Berg and M. C. Kiernan, *Nat. Rev. Neurol.*, 2011, **7**, 639–649.

4 W. Robberecht and T. Philips, *Nat. Rev. Neurosci.*, 2013, **14**, 248–264.

5 D. R. Rosen, T. Siddique, D. Patterson, D. A. Figlewicz, P. Sapp, A. Hentati, D. Donaldson, J. Goto, J. P. O'Regan, H.-X. Deng, Z. Rahmani, A. Krizus, D. McKenna-Yasek, A. Cayabyab, S. M. Gaston, R. Berger, R. E. Tanzi, J. J. Halperin, B. Herzfeldt, R. Van den Bergh, W.-Y. Hung, T. Bird, G. Deng, D. W. Mulder, C. Smyth, N. G. Laing, E. Soriano, M. A. Pericak–Vance, J. Haines, G. A. Rouleau, J. S. Gusella, H. R. Horvitz and R. H. Brown, *Nature*, 1993, **362**, 59–62.

6 P. M. Andersen, *Curr. Neurol. Neurosci. Rep.*, 2006, **6**, 37–46.

7 M. Cozzolino, A. Ferri and M. T. Carrì, *Antioxid. Redox Signal.*, 2008, **10**, 405–443.

8 M. Gurney, H. Pu, A. Chiu, M. Dal Canto, C. Polchow, D. Alexander, J. Caliendo, A. Hentati, Y. Kwon, H. Deng and A. Et, *Science (80-.).*, 1994, **264**, 1772–1775.

9 L. I. Bruijn, M. K. Houseweart, S. Kato, K. L. Anderson, S. D. Anderson, E. Ohama, A. G. Reaume, R. W. Scott and D. W. Cleveland, *Science*, 1998, **281**, 1851–4.

10 L. I. Bruijn, M. W. Becher, M. K. Lee, K. L. Anderson, N. A. Jenkins, N. G. Copeland, S. S. Sisodia, J. D. Rothstein, D. R. Borchelt, D. L. Price and D. W. Cleveland, *Neuron*, 1997, **18**, 327–38.

11 M. E. Ripps, G. W. Huntley, P. R. Hof, J. H. Morrison and J. W. Gordon, *Proc. Natl. Acad. Sci. U. S. A.*, 1995, **92**, 689–93.

12 S. Saxena, E. Cabuy and P. Caroni, *Nat. Neurosci.*, 2009, **12**, 627–36.

13 M. T. Carri, A. Battistoni, F. Polizio, A. Desideri and G. Rotilio, *FEBS Lett.*, 1994, **356**, 314–6.

14 W. S. Eum and J. H. Kang, *Mol. Cells*, 1999, **9**, 110–4.

15 L. J. Hayward, J. a Rodriguez, J. W. Kim, A. Tiwari, J. J. Goto, D. E. Cabelli, J. S. Valentine and R. H. Brown, *J. Biol. Chem.*, 2002, **277**, 15923–31.

16 L. Gaetke, *Toxicology*, 2003, **189**, 147–163.

17 M. Valko, H. Morris and M. Cronin, *Curr. Med. Chem.*, 2005, **12**, 1161–1208.

18 K. Jomova and M. Valko, *Toxicology*, 2011, **283**, 65–87.

19 D. Hare, S. Ayton, A. Bush and P. Lei, *Front. Aging Neurosci.*, 2013, **5**, 34.

20 H. Tapiero, D. M. Townsend and K. D. Tew, *Biomed. Pharmacother.*, 2003, **57**, 386–398.

21 K. M. Davies, S. Bohic, A. Carmona, R. Ortega, V. Cottam, D. J. Hare, J. P. M. Finberg, S. Reyes, G. M. Halliday, J. F. B. Mercer and K. L. Double, *Neurobiol. Aging*, 2014, **35**, 858–866.

22 F. Larner, B. Sampson, M. Rehkämper, D. J. Weiss, J. R. Dainty, S. O'Riordan, T. Panetta and P. G. Bain, *Metallomics*, 2013, **5**, 125.

23 P. Dusek, P. M. Roos, T. Litwin, S. A. Schneider, T. P. Flaten and J. Aaseth, *J. Trace Elem. Med. Biol.*, 2015, **31**, 193–203.

24 M. a Greenough, J. Camakaris and A. I. Bush, *Neurochem. Int.*, 2013, **62**, 540–55.

25 E. House, M. Esiri, G. Forster, P. G. Ince and C. Exley, *Metallomics*, 2012, **4**,

56–65.
26 D. Kaden, A. I. Bush, R. Danzeisen, T. A. Bayer and G. Multhaup, *Int. J. Alzheimers. Dis.*, 2011, **2011**, 345614.
27 D. Shore, R. I. Henkin, N. R. Nelson, R. P. Agarwal and R. J. Wyatt, *J. Am. Geriatr. Soc.*, 1984, **32**, 892–895.
28 B. R. Roberts, N. K. H. Lim, E. J. McAllum, P. S. Donnelly, D. J. Hare, P. a Doble, B. J. Turner, K. a Price, S. Chun Lim, B. M. Paterson, J. L. Hickey, T. W. Rhoads, J. R. Williams, K. M. Kanninen, L. W. Hung, J. R. Liddell, A. Grubman, J.-F. Monty, R. M. Llanos, D. R. Kramer, J. F. B. Mercer, A. I. Bush, C. L. Masters, J. a Duce, Q.-X. Li, J. S. Beckman, K. J. Barnham, A. R. White and P. J. Crouch, *J. Neurosci.*, 2014, **34**, 8021–8031.
29 P. M. Roos, O. Vesterberg, T. Syversen, T. P. Flaten and M. Nordberg, *Biol. Trace Elem. Res.*, 2013, **151**, 159–70.
30 I. Hozumi, T. Hasegawa, A. Honda, K. Ozawa, Y. Hayashi, K. Hashimoto, M. Yamada, A. Koumura, T. Sakurai, A. Kimura, Y. Tanaka, M. Satoh and T. Inuzuka, *J. Neurol. Sci.*, 2011, **303**, 95–99.
31 Q.-X. Li, S. S. Mok, K. M. Laughton, C. a McLean, I. Volitakis, R. a Cherny, N. S. Cheung, A. R. White and C. L. Masters, *Aging Cell*, 2006, **5**, 153–65.
32 E. Tokuda, E. Okawa, S. Watanabe, S.-I. Ono and S. L. Marklund, *Neurobiol. Dis.*, 2013, **54**, 308–319.
33 E. Tokuda, E. Okawa, S. Watanabe and S.-I. Ono, *Hum. Mol. Genet.*, 2014, **23**, 1271–85.
34 E. Tokuda, S. Watanabe, E. Okawa and S. Ono, *Neurotherapeutics*, 2015, **12**, 461–476.
35 E. Tokuda, S. Ono, K. Ishige, S. Watanabe, E. Okawa, Y. Ito and T. Suzuki, *Exp. Neurol.*, 2008, **213**, 122–8.
36 E. Tokuda, S. I. Ono, K. Ishige, A. Naganuma, Y. Ito and T. Suzuki, *Toxicology*, 2007, **229**, 33–41.
37 E. Tokuda, E. Okawa and S. I. Ono, *J. Neurochem.*, 2009, **111**, 181–191.
38 M. W. Bourassa, H. H. Brown, D. R. Borchelt, S. Vogt and L. M. Miller, *Front. Aging Neurosci.*, 2014, **6**, 1–6.
39 M. W. Bourassa and L. M. Miller, *Metallomics*, 2012, **4**, 721.
40 H. L. Lelie, A. Liba, M. W. Bourassa, M. Chattopadhyay, P. K. Chan, E. B. Gralla, L. M. Miller, D. R. Borchelt, J. S. Valentine and J. P. Whitelegge, *J. Biol. Chem.*, 2011, **286**, 2795–2806.
41 T. N. T. Dang, N. K. H. Lim, A. Grubman, Q.-X. Li, I. Volitakis, A. R. White and P. J. Crouch, *Front. Aging Neurosci.*, 2014, **6**, 15.
42 K. Ikeda, T. Hirayama, T. Takazawa, K. Kawabe and Y. Iwasaki, *Intern. Med.*, 2012, **51**, 1501–1508.
43 Y. Nadjar, P. Gordon, P. Corcia, G. Bensimon, L. Pieroni, V. Meininger and F. Salachas, *PLoS One*, 2012, **7**, 2–7.
44 X. W. Su, S. L. Clardy, H. E. Stephens, Z. Simmons and J. R. Connor, *Amyotroph. Lateral Scler. Front. Degener.*, 2015, **16**, 102–107.
45 E. F. Goodall, M. S. Haque and K. E. Morrison, *J. Neurol.*, 2008, **255**, 1652–1656.
46 C. Langkammer, C. Enzinger, S. Quasthoff, P. Grafenauer, M. Soellinger, F. Fazekas and S. Ropele, *J. Magn. Reson. Imaging*, 2010, **31**, 1339–1345.
47 J. Y. Kwan, S. Y. Jeong, P. van Gelderen, H. X. Deng, M. M. Quezado, L. E. Danielian, J. A. Butman, L. Chen, E. Bayat, J. Russell, T. Siddique, J. H. Duyn, T. A. Rouault and M. K. Floeter, *PLoS One*, 2012, **7**.

48 A. Ignjatović, Z. Stević, S. Lavrnić, M. Daković and G. Bačić, *J. Magn. Reson. Imaging*, 2013, **38**, 1472–1479.

49 A. Ignjatović, Z. Stević, D. Lavrnić, A. Nikolić-Kokić, D. Blagojević, M. Spasić and I. Spasojević, *Amyotroph. Lateral Scler.*, 2012, **13**, 357–362.

50 S. Oshiro, M. S. Morioka and M. Kikuchi, *Adv. Pharmacol. Sci.*, 2011, **2011**, 1–8.

51 T. D. B. Lyon and G. S. Fell, *J. Anal. At. Spectrom.*, 1990, **5**, 135.

52 T. D. B. Lyon, S. Fletcher, G. S. Fell and M. Patriarca, *Microchem. J.*, 1996, **54**, 236–245.

53 J. R. Turnlund, M. C. Michel, W. R. Keyes, Y. Schutz and S. Margen, *Am. J. Clin. Nutr.*, 1982, **36**, 587–91.

54 J. R. Turnlund, W. R. Keyes, H. L. Anderson and L. L. Acord, *Am. J. Clin. Nutr.*, 1989, **49**, 870–8.

55 L. J. Harvey, J. R. Dainty, W. J. Hollands, V. J. Bull, J. H. Beattie, T. I. Venelinov, J. A. Hoogewerff, I. M. Davies and S. J. Fairweather-Tait, *Use of mathematical modeling to study copper metabolism in humans.*, 2005, vol. 81.

56 F. Albarède, *Elements*, 2015, **11**, 265–269.

57 J. Bigeleisen and M. G. Mayer, *J. Chem. Phys.*, 1947, **15**, 261.

58 V. Balter, A. Lamboux, A. Zazzo, P. Télouk, Y. Leverrier, J. Marvel, A. P. Moloney, F. J. Monahan, O. Schmidt and F. Albarède, *Metallomics*, 2013, **5**, 1470.

59 V. Balter, A. Nogueira da Costa, V. P. Bondanese, K. Jaouen, A. Lamboux, S. Sangrajrang, N. Vincent, F. Fourel, P. Télouk, M. Gigou, C. Lécuyer, P. Srivatanakul, C. Bréchot, F. Albarède and P. Hainaut, *Proc. Natl. Acad. Sci.*, 2015, **112**, 982–985.

60 F. Albarede, P. Télouk, V. Balter, V. P. Bondanese, E. Albalat, P. Oger, P. Bonaventura, P. Miossec and T. Fujii, *Metallomics*, 2016, **8**, 1056–1070.

61 J. L. L. Morgan, G. W. Gordon, R. C. Arrua, J. L. Skulan, A. D. Anbar and T. D. Bullen, *Anal. Chem.*, 2011, **83**, 6956–6962.

62 J. L. L. Morgan, J. L. Skulan, G. W. Gordon, S. J. Romaniello, S. M. Smith and A. D. Anbar, *Proc. Natl. Acad. Sci.*, 2012, **109**, 9989–9994.

63 P. Télouk, A. Puisieux, T. Fujii, V. Balter, V. P. Bondanese, A.-P. Morel, G. Clapisson, A. Lamboux and F. Albarede, *Metallomics*, 2015, **7**, 299–308.

64 M. Costas-Rodríguez, Y. Anoshkina, S. Lauwens, H. Van Vlierberghe, J. Delanghe and F. Vanhaecke, *Metallomics*, 2015, **7**, 491–498.

65 F. Larner, L. N. Woodley, S. Shousha, A. Moyes, E. Humphreys-Williams, S. Strekopytov, A. N. Halliday, M. Rehkämper and R. C. Coombes, *Metallomics*, 2015, **7**, 112–117.

66 F. Larner, S. Shousha and R. C. Coombes, *Biomark. Med.*, 2015, **9**, 379–382.

67 M. Costas-Rodríguez, J. Delanghe and F. Vanhaecke, *TrAC Trends Anal. Chem.*, 2016, **76**, 182–193.

68 M. K. Olsen, S. L. Roberds, B. R. Ellerbrock, T. J. Fleck, D. K. McKinley and M. E. Gurney, *Ann. Neurol.*, 2001, **50**, 730–40.

69 T. G. Enge, M. P. Field, D. F. Jolley, H. Ecroyd, M. H. Kim and A. Dosseto, *J. Anal. At. Spectrom.*, 2016, **31**, 2023–2030.

70 F. Larner, M. Rehkämper, B. J. Coles, K. Kreissig, D. J. Weiss, B. Sampson, C. Unsworth and S. Strekopytov, *J. Anal. At. Spectrom.*, 2011, **26**, 1627.

71 D. C. Baxter, I. Rodushkin, E. Engström and D. Malinovsky, *J. Anal. At. Spectrom.*, 2006, **21**, 427.

72 S. G. Nielsen, M. Rehkämper, J. Baker and A. N. Halliday, *Chem. Geol.*, 2004,

204, 109–124.
73 X. K. Zhu, R. K. O'Nions, Y. Guo, N. S. Belshaw and D. Rickard, *Chem. Geol.*, 2000, **163**, 139–149.
74 R Core Team, 2016.
75 D. J. Barr, R. Levy, C. Scheepers and H. J. Tily, *J. Mem. Lang.*, 2013, **68**, 255–278.
76 D. R. Borchelt, M. K. Lee, H. S. Slunt, M. Guarnieri, Z. S. Xu, P. C. Wong, R. H. Brown, D. L. Price, S. S. Sisodia and D. W. Cleveland, *Proc. Natl. Acad. Sci. U. S. A.*, 1994, **91**, 8292–6.
77 J. B. Hilton, A. R. White and P. J. Crouch, *J. Mol. Med.*, 2015, **93**, 481–487.
78 A. F. Hottinger, E. G. Fine, M. E. Gurney, A. D. Zurn and P. Aebischer, *Eur. J. Neurosci.*, 1997, **9**, 1548–1551.
79 S. Nagano, Y. Fujii, T. Yamamoto, M. Taniyama, K. Fukada, T. Yanagihara and S. Sakoda, *Exp. Neurol.*, 2003, **179**, 176–80.
80 A. G. Estévez, J. P. Crow, J. B. Sampson, C. Reiter, Y. Zhuang, G. J. Richardson, M. M. Tarpey, L. Barbeito and J. S. Beckman, *Science*, 1999, **286**, 2498–500.
81 N. T. Davies and T. Davies, *Proc Nutr Soc*, 1974, **33**, 293–298.
82 E. Tokuda and Y. Furukawa, *Int. J. Mol. Sci.*, 2016, **17**, 636.
83 G. S. A. Wright, S. V. Antonyuk and S. S. Hasnain, *Sci. Rep.*, 2016, **6**, 27691.
84 J. B. Hilton, A. R. White and P. J. Crouch, *Metallomics*, 2016, **8**, 1002–1011.
85 E. J. McAllum, N. K.-H. Lim, J. L. Hickey, B. M. Paterson, P. S. Donnelly, Q.-X. Li, J. R. Liddell, K. J. Barnham, A. R. White and P. J. Crouch, *Amyotroph. Lateral Scler. Frontotemporal Degener.*, 2013, **14**, 586–90.
86 G. W. Evans, *Physiol. Rev.*, 1973, **53**, 535–70.
87 B. A. Neel, Y. Lin and J. E. Pessin, *Trends Endocrinol. Metab.*, 2013, **24**, 635–643.
88 M. C. Linder, *Biochemistry of Copper*, Springer US, Boston, MA, 1991.
89 G. Luo, J. Yi, C. Ma, Y. Xiao, F. Yi, T. Yu and J. Zhou, *PLoS One*, 2013, **8**, e82112.
90 J.-L. Gonzalez de Aguilar, C. Niederhauser-Wiederkehr, B. Halter, M. De Tapia, F. Di Scala, P. Demougin, L. Dupuis, M. Primig, V. Meininger and J.-P. Loeffler, *Physiol. Genomics*, 2008, **32**, 207–218.
91 Y. Xiao, C. Ma, J. Yi, S. Wu, G. Luo, X. Xu, P.-H. Lin, J. Sun and J. Zhou, *Physiol. Rep.*, 2015, **3**, e12271–e12271.
92 S. Boillée, C. Vande Velde and D. Cleveland, *Neuron*, 2006, **52**, 39–59.
93 M. C. Kiernan, S. Vucic, B. C. Cheah, M. R. Turner, A. Eisen, O. Hardiman, J. R. Burrell and M. C. Zoing, *Lancet*, 2011, **377**, 942–55.
94 L. R. Fischer, D. G. Culver, P. Tennant, A. a. Davis, M. Wang, A. Castellano-Sanchez, J. Khan, M. a. Polak and J. D. Glass, *Exp. Neurol.*, 2004, **185**, 232–40.
95 D. Frey, C. Schneider, L. Xu, J. Borg, W. Spooren and P. Caroni, *J. Neurosci.*, 2000, **20**, 2534–42.
96 J. Zhou, J. Yi and L. Bonewald, *Curr. Osteoporos. Rep.*, 2015, **13**, 274–279.
97 Q. T. Nguyen, Y. J. Son, J. R. Sanes and J. W. Lichtman, *J. Neurosci.*, 2000, **20**, 6077–86.
98 T. Domzał and B. Radzikowska, *Neurol. Neurochir. Pol.*, 1983, **17**, 343–6.
99 E. Kapaki, C. Zournas, G. Kanias, T. Zambelis, A. Kakami and C. Papageorgiou, *J. Neurol. Sci.*, 1997, **147**, 171–175.
100 R. Pamphlett, R. McQuilty and K. Zarkos, *Neurotoxicology*, 2001, **22**, 401–

410.
101 A. Cabrera, E. Alonzo, E. Sauble, Y. L. Chu, D. Nguyen, M. C. Linder, D. S. Sato and A. Z. Mason, *BioMetals*, 2008, **21**, 525–543.
102 A. Montaser, C. Tetreault and M. Linder, *Exp. Biol. Med.*, 1992, **200**, 321–329.
103 T. L. Peters, J. D. Beard, D. M. Umbach, K. Allen, J. Keller, D. Mariosa, D. P. Sandler, S. Schmidt, F. Fang, W. Ye and F. Kamel, *Neurotoxicology*, 2016, **54**, 119–126.
104 E. A. Schauble, *Rev. Mineral. Geochemistry*, 2004, **55**, 65–111.
105 V. P. Bondanese, A. Lamboux, M. Simon, J. Lafont, E. Albalat, S. Pichat, J.-M. Vanacker, P. Télouk, V. Balter, P. Oger and F. Albarède, *Metallomics*, 2016.
106 R. J. Ferrante, S. E. Browne, L. A. Shinobu, A. C. Bowling, M. J. Baik, U. MacGarvey, N. W. Kowall, R. H. Brown and M. F. Beal, *J. Neurochem.*, 1997, **69**, 2064–74.
107 E. Gordillo, A. Ayala, J. Bautista and A. Machado, *J. Biol. Chem.*, 1989, **264**, 17024–8.
108 J. M. Matés and F. Sánchez-Jiménez, *Front. Biosci.*, 1999, **4**, D339-45.
109 L. M. Sayre, M. A. Smith and G. Perry, *Curr. Med. Chem.*, 2001, **8**, 721–38.
110 E. Stadtman, *Science (80-.).*, 1992, **257**, 1220–1224.
111 I. Niebrój-Dobosz, D. Dziewulska and H. Kwieciński, *Folia Neuropathol.*, 2004, **42**, 151–6.
112 L. Ferraiuolo, J. Kirby, A. J. Grierson, M. Sendtner and P. J. Shaw, *Nat. Rev. Neurol.*, 2011, **7**, 616–630.
113 J. Prousek, *Pure Appl. Chem.*, 2007, **79**.
114 H. Speisky, M. Gómez, F. Burgos-Bravo, C. López-Alarcón, C. Jullian, C. Olea-Azar and M. E. Aliaga, *Bioorg. Med. Chem.*, 2009, **17**, 1803–10.
115 M. D. Mattie and J. H. Freedman, *Am. J. Physiol. Cell Physiol.*, 2004, **286**, C293-301.
116 A. Ahuja, K. Dev, R. S. Tanwar, K. K. Selwal and P. K. Tyagi, *J. Trace Elem. Med. Biol.*, 2015, **29**, 11–23.
117 L. Siklós, J. I. Engelhardt, M. E. Alexianu, M. E. Gurney, T. Siddique and S. H. Appel, *J. Neuropathol. Exp. Neurol.*, 1998, **57**, 571–87.
118 R. H. Swerdlow, J. K. Parks, G. Pattee and w davis P. Jr, *Amyotroph. Lateral Scler. Other Mot. Neuron Disord.*, 2000, **1**, 185–190.
119 S. C. Barber, R. J. Mead and P. J. Shaw, *Biochim. Biophys. Acta - Mol. Basis Dis.*, 2006, **1762**, 1051–1067.
120 S. C. Barber and P. J. Shaw, *Free Radic. Biol. Med.*, 2010, **48**, 629–41.
121 R. Liu, J. S. Althaus, B. R. Ellerbrock, D. A. Becker and M. E. Gurney, *Ann. Neurol.*, 1998, **44**, 763–70.
122 J. R. Prohaska and A. A. Gybina, *J. Nutr.*, 2004, **134**, 1003–6.
123 P. C. Wong, C. a Pardo, D. R. Borchelt, M. K. Lee, N. G. Copeland, N. a Jenkins, S. S. Sisodia, D. W. Cleveland and D. L. Price, *Neuron*, 1995, **14**, 1105–16.
124 A. Henriques, C. Pitzer and A. Schneider, *PLoS One*, 2010, **5**, e15445.
125 B.-S. Choi and W. Zheng, *Brain Res.*, 2009, **1248**, 14–21.
126 J. R. Mann, J. Camakaris and D. M. Danks, *Biochem. J.*, 1979, **180**, 613–9.
127 M. Wong and L. J. Martin, *Hum. Mol. Genet.*, 2010, **19**, 2284–302.
128 H. Basun, L. G. Forssell, L. Wetterberg and B. Winblad, *J. Neural Transm. Park. Dis. Dement. Sect.*, 1991, **3**, 231–258.
129 L. Zecca, M. Gallorini, V. Schünemann, A. X. Trautwein, M. Gerlach, P.

Riederer, P. Vezzoni and D. Tampellini, *J. Neurochem.*, 2001, **76**, 1766–1773.
130 K. Flurkey, J. McCurrer and D. Harrison, in *The Mouse in Biomedical Research*, Elsevier, 2007, pp. 637–672.
131 S. Horvath, *Genome Biol.*, 2013, **14**, R115.
132 P. E. Johnson, D. B. Milne and G. I. Lykken, *Am. J. Clin. Nutr.*, 1992, **56**, 917–25.
133 J. R. Turnlund, *Am. J. Clin. Nutr.*, 1998, **67**, 960S–964S.
134 L. Gambling, R. Danzeisen, C. Fosset, H. S. Andersen, S. Dunford, S. K. S. Srai and H. J. MCArdle, *J. Nutr.*, 2003, **133**, 1554S–6S.
135 S. a Donley, B. J. Ilagan, H. Rim and M. C. Linder, *Am. J. Physiol. Endocrinol. Metab.*, 2002, **283**, E667–E675.
136 R. Uauy, M. Olivares and M. Gonzalez, *Am. J. Clin. Nutr.*, 1998, **67**, 952S–959S.
137 K. K. Tong and H. J. McArdle, *Biochim. Biophys. Acta - Mol. Cell Res.*, 1995, **1269**, 233–236.
138 H. J. McArdle and G. J. van den Berg, *J. Nutr.*, 1992, **122**, 1260–5.
139 M. C. Linder, C. A. Goode, K. C. Weiss, P.-L. Wirth and M. H. Vu, in *Metabolism of Minerals and Trace Elements in Human Disease*, eds. M. Abdulla, H. Dashti, B. Sarkar, H. Al-Sayer and N. Al-Naqeeb, Smith-Gordon, London, 1989.
140 G. Crisponi, V. M. Nurchi, D. Fanni, C. Gerosa, S. Nemolato and G. Faa, *Coord. Chem. Rev.*, 2010, **254**, 876–889.

Table of Contents:

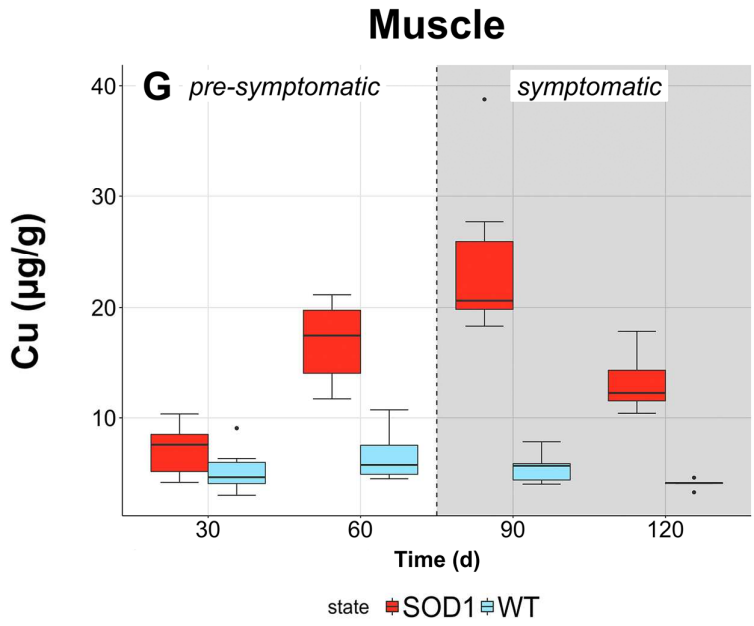

Muscle tissue may play an important role in the aetiology of amyotrophic lateral sclerosis, where accumulation in the tissue may aid in the development of the disease.

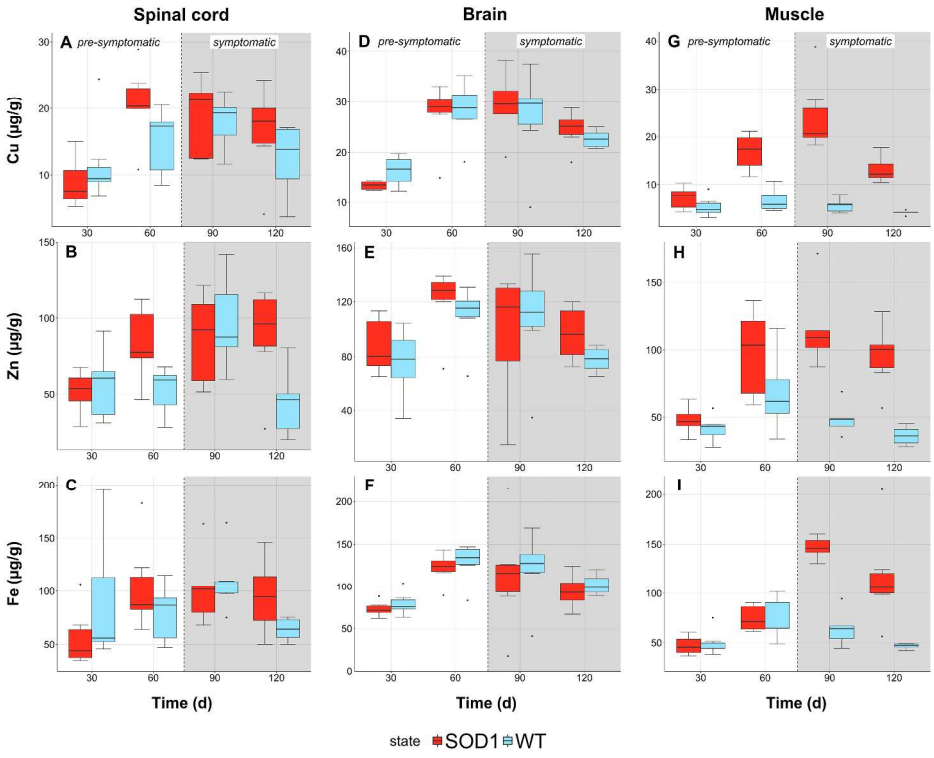

Figure 1: Copper (A-C), Zn (D-F) and Fe (G-I) concentrations in spinal cord, brain and muscle tissue (µg g-1 of dry tissue) as a function of time (days). Elevated concentrations of Cu, Zn and Fe are evident in muscle tissue and appear to precede the development of symptoms in Cu, while Zn and Fe are trailing the development of symptoms. Box plots show median values (solid horizontal line, 50th percentile (box outline), 90th percentile (whiskers) and outlier values (filled circles); n ≥ 5.

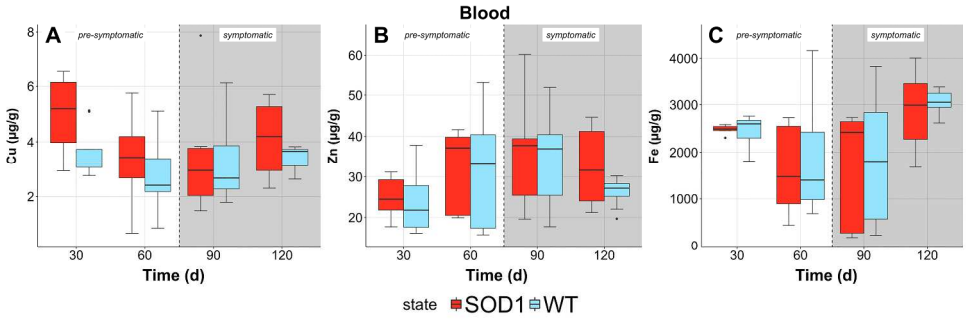

Figure 2: Copper (A), Zn (B) and Fe (C) concentrations in whole blood (µg g-1 of dry tissue) as a function of time (days). Box plots show median values (solid horizontal line, 50th percentile (box outline), 90th percentile (whiskers) and outlier values (filled circles); n ≥ 6.

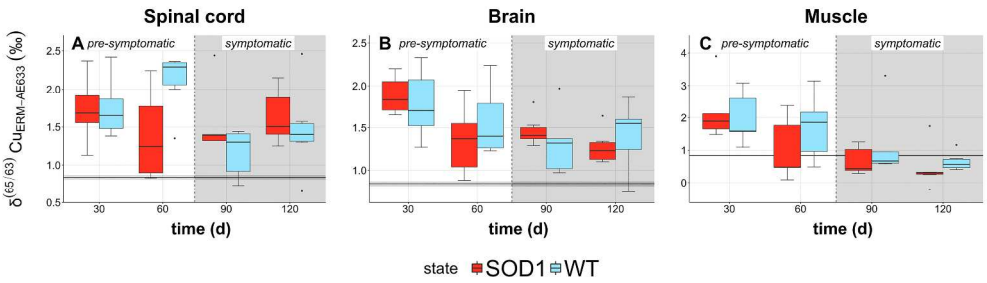

Figure 3: Copper isotope ratios in spinal cord (A), brain (B) and muscle tissue (C), as a function of time (in days). The gray line indicates the Cu isotope ratio of food (0.84 ± 0.03‰; ±2SE). Box plots show median values (solid horizontal line, 50th percentile (box outline), 90th percentile (whiskers) and outlier values (filled circles); n ≥ 6.

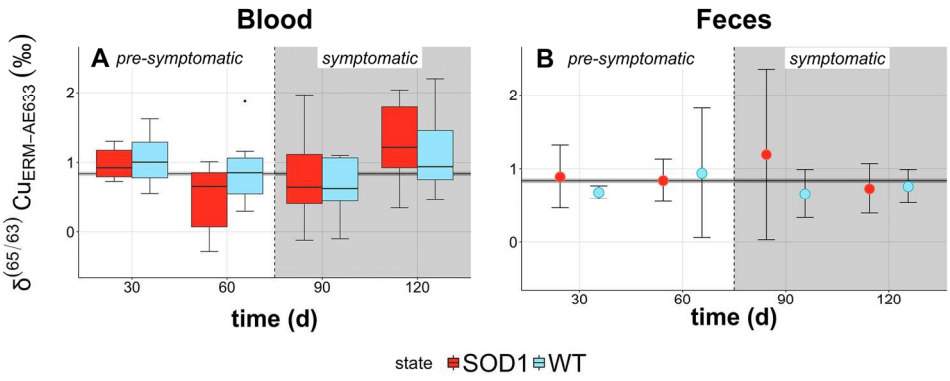

Figure 4: Copper isotope ratios in whole blood and feces against time (d), including food (gray line; 0.84 ± 0.03‰; ±2SE). Box plots (A) show median values (solid horizontal line, 50th percentile (box outline), 90th percentile (whiskers) and outlier values (filled circles) (n ≥ 7). Results in plot B show mean ± 2SE (n = 6).

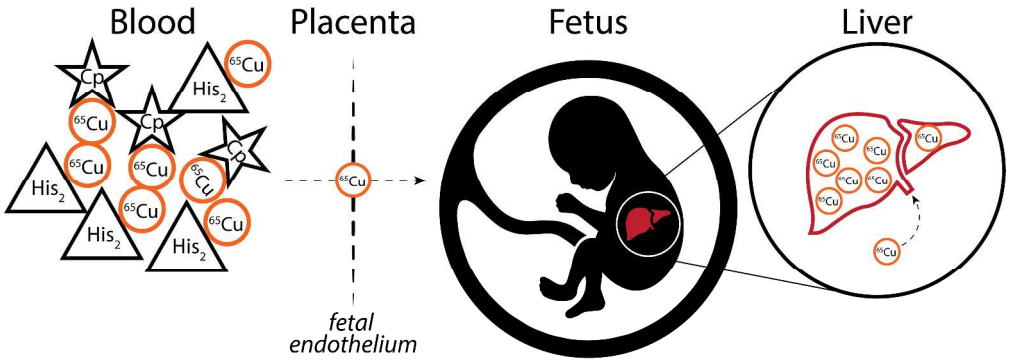

Figure 5: Uptake of Cu into the fetus via the placenta. Ceruloplasmin, and other low molecular copper-compounds, predominantly $[Cu^{2+}(His)_2]$, accumulate the heavy isotope ^{65}Cu. This Cu then accumulates in the liver of the fetus after crossing the fetal endothelium, enriching it in ^{65}Cu.

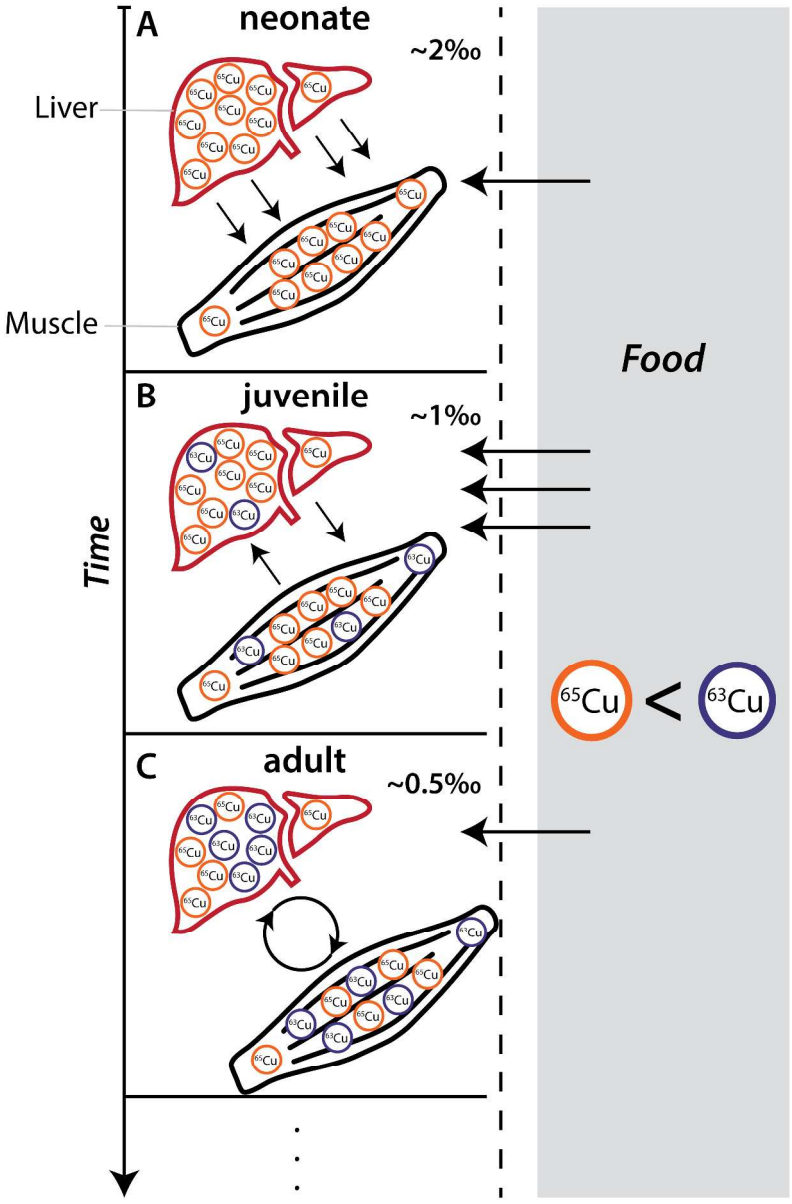

Figure 6: Conceptual model for the presence of a 'starting pool' of heavy Cu received from the mother and accumulated in the fetal liver (A). This Cu is an initial source for the fast neonatal growth phase, distributing ^{65}Cu throughout the tissues. The commencement of ingestion of external non-maternal food (lighter Cu isotopic composition) meets the high nutrient requirement of juvenile growth (B). This dilutes the pre-existing heavy Cu pool. The dilution continues until adult-hood, at which point growth stops and Cu isotope ratios stabilize, reflecting the food's isotope ratio (C). At this point, localized recycling processes with endogenic and exogenic Cu are possible.

Supplementary information:

Results of the linear model with the following parameters:
Dependent variables: Cu, Zn, Fe, CuIso (Cu isotope ratios)
Independent variables: time (30, 60, 90, 120) and state (SOD1 and WT)
Time was treated as a continuous variable.
stateWT is the indicator variable for difference between states, with *stateSOD1* being the reference.

Results:

Cu
Cu Brain

Coefficients:

	Estimate	Std. Error	t value	Pr(>|t|)	
(Intercept)	16.88036	2.62173	6.439	6.96e-08	***
stateWT	-0.10929	2.00551	-0.054	0.95678	
time	0.08835	0.02940	3.005	0.00434	**

Cu Spinal cord

Coefficients:

	Estimate	Std. Error	t value	Pr(>|t|)	
(Intercept)	12.82288	2.35142	5.453	2.01e-06	***
stateWT	-1.89467	1.79873	-1.053	0.298	
time	0.04401	0.02637	1.669	0.102	

Cu Muscle

Coefficients:

	Estimate	Std. Error	t value	Pr(>|t|)	
(Intercept)	12.75008	2.15083	5.928	4.31e-07	***
stateWT	-10.00600	1.64097	-6.098	2.43e-07	***
time	0.03469	0.02425	1.430	0.16	

Cu blood

Coefficients:

	Estimate	Std. Error	t value	Pr(>|t|)	
(Intercept)	4.202613	0.512487	8.200	3.62e-11	***
stateWT	-0.674357	0.375417	-1.796	0.0778	.
time	-0.003440	0.005556	-0.619	0.5383	

Zn

Zn Brain

Coefficients:

	Estimate	Std. Error	t value	Pr(>|t|)	
(Intercept)	98.20885	11.56640	8.491	6.73e-11	***
stateWT	-7.97077	8.84776	-0.901	0.372	
time	0.02585	0.12972	0.199	0.843	

Zn Spinal cord

Coefficients:

	Estimate	Std. Error	t value	Pr(>|t|)	
(Intercept)	60.0657	10.9858	5.468	2.03e-06	***
stateWT	-13.4311	8.3714	-1.604	0.1158	
time	0.2311	0.1240	1.864	0.0691	.

Zn Muscle

Coefficients:

	Estimate	Std. Error	t value	Pr(>|t|)	
(Intercept)	72.8489	10.7452	6.780	2.68e-08	***
stateWT	-39.3087	8.2716	-4.752	2.27e-05	***
time	0.2055	0.1212	1.695	0.0973	.

Zn blood

Coefficients:

	Estimate	Std. Error	t value	Pr(>|t|)	
(Intercept)	26.34043	3.48919	7.549	3.5e-10	***
stateWT	-2.50953	2.62022	-0.958	0.342	
time	0.06186	0.03827	1.617	0.111	

Fe

Fe Brain

Coefficients:

	Estimate	Std. Error	t value	Pr(>|t|)	
(Intercept)	107.82885	21.05521	5.121	1.52e-05	***
stateWT	5.84396	13.38300	0.437	0.665	
time	0.01305	0.23155	0.056	0.955	

Fe Spinal cord

Coefficients:

	Estimate	Std. Error	t value	Pr(>|t|)	
(Intercept)	79.4316	15.0040	5.294	3.63e-06	***
stateWT	-1.9171	11.4334	-0.168	0.868	
time	0.1296	0.1693	0.766	0.448	

Fe Muscle

Coefficients:

	Estimate	Std. Error	t value	Pr(>|t|)	
(Intercept)	62.3861	12.2794	5.081	7.77e-06	***
stateWT	-35.3730	9.4527	-3.742	0.000536	***
time	0.4231	0.1385	3.054	0.003871	**

Fe blood

Coefficients:

	Estimate	Std. Error	t value	Pr(>|t|)	
(Intercept)	1478.196	360.696	4.098	0.000129	***
stateWT	152.990	269.184	0.568	0.571956	
time	7.907	3.954	2.000	0.050130	.

CuIso

CuIso Brain

Coefficients:

	Estimate	Std. Error	t value	Pr(>|t|)	
(Intercept)	1.939807	0.198597	9.768	8.55e-13	***
stateWT	-0.078462	0.150649	-0.521	0.6047	
time	-0.005942	0.002227	-2.669	0.0105	*

CuIso Spinal cord

Coefficients:

	Estimate	Std. Error	t value	Pr(>|t|)	
(Intercept)	1.81947	0.18462	9.855	6.46e-13	***
stateWT	0.01631	0.13995	0.117	0.908	
time	-0.00291	0.00207	-1.406	0.167	**

CuIso Muscle

Coefficients:

	Estimate	Std. Error	t value	Pr(>|t|)	
(Intercept)	2.327292	0.303983	7.656	1.10e-09	***
stateWT	0.287917	0.229790	1.253	0.217	
time	-0.016758	0.003426	-4.892	1.32e-05	***

CuIso blood

Coefficients:

	Estimate	Std. Error	t value	Pr(>|t|)	
(Intercept)	0.8819047	0.2003504	4.402	4.4e-05	***
stateWT	-0.0017195	0.1488245	-0.012	0.991	
time	0.0008823	0.0022175	0.398	0.692	